14 Sep 2021

Evolutionary Algorithm-Based Adaptive Robust Optimization for AC Security Constrained Unit Commitment Considering Renewable Energy Sources and Shunt Facts Devices

Aliasghar Baziar

Rui Bo
Missouri University of Science and Technology, rbo@mst.edu

Misagh Dehghani Ghotbabadi

Mehdi Veisi

et. al. For a complete list of authors, see https://scholarsmine.mst.edu/ele_comeng_facwork/4446

Recommended Citation

A. Baziar et al., "Evolutionary Algorithm-Based Adaptive Robust Optimization for AC Security Constrained Unit Commitment Considering Renewable Energy Sources and Shunt Facts Devices," *IEEE Access*, vol. 9, pp. 123575-123587, Institute of Electrical and Electronics Engineers (IEEE), Sep 2021.
The definitive version is available at https://doi.org/10.1109/ACCESS.2021.3108763

IEEE Access
Multidisciplinary | Rapid Review | Open Access Journal

Received July 10, 2021, accepted July 19, 2021, date of publication August 30, 2021, date of current version September 14, 2021.

Digital Object Identifier 10.1109/ACCESS.2021.3108763

Evolutionary Algorithm-Based Adaptive Robust Optimization for AC Security Constrained Unit Commitment Considering Renewable Energy Sources and Shunt FACTS Devices

ALIASGHAR BAZIAR[1], RUI BO[1], (Senior Member, IEEE), MISAGH DEHGHANI GHOTBABADI[2], MEHDI VEISI[3], AND WAQAS UR REHMAN[1], (Graduate Student Member, IEEE)

[1]Department of Electrical and Computer Engineering, Missouri University of Science and Technology, Rolla, MO 65409, USA
[2]Department of Electrical Engineering, Mapna Operation and Maintenance Company, Tehran 1919613871, Iran
[3]Sama Technical and Vocational Training College Tehran Branch (Tehran), Islamic Azad University, Tehran 1381148143, Iran

Corresponding author: Rui Bo (rbo@mst.edu)

ABSTRACT An AC security constrained unit commitment (AC-SCUC) in the presence of the renewable energy sources (RESs) and shunt flexible AC transmission system (FACTS) devices is conventionally modeled as a deterministic optimization problem to minimize the operation cost of conventional generation units (CGUs) subject to AC optimal power flow (AC-OPF) equations, operation constraints of RESs, shunt FACTS devices, and CGUs. To cope with the uncertainties of load and RES generation, robust and stochastic optimization and linearized formulation have been used to achieve a sub-optimal solution. To arrive at a more optimal solution, an evolutionary algorithm-based adaptive robust optimization (EA-ARO) approach to solve the non-linear and non-convex optimization problem was proposed. A hybrid solver of grey wolf optimization (GWO) and teaching learning-based optimization (TLBO) was proposed to solve the AC-SCUC problem in the worst-case scenario to obtain robust and reliable optimal solution. Finally, the proposed method was simulated on standard IEEE test systems to demonstrate its capabilities, and the results showed the proposed hybrid solver obtained robust optimal solutions with reduced computation time and standard deviation. Moreover, the numerical results proved the proposed strategy's capabilities of improving the economics of generation units, such as lower operational cost, and enhancing the performance of the transmission networks, such as improved voltage profile and reduced energy losses.

INDEX TERMS AC security constrained unit commitment, evolutionary algorithm, adaptive robust optimization, shunt FACTS devices, renewable energy sources.

NOMENCLATURE

INDICES AND SETS

n, j, g, t, κ, l, f	Indices of bus, bus, CGU, time, RES, load, and shunt FACT
$\Upsilon_N, \Upsilon_G, \Upsilon_T, \Upsilon_R, \Upsilon_L, \Upsilon_F$	Set of bus, CGU, time, RES, load, and shunt FACT

VARIABLES

$Cost$	The cost function of CGUs ($)
f_1, f_2	Auxiliary functions in per unit (p.u.)
P^G, Q^G, R^G	Active power, reactive power, and reserve of the CGU (p.u.)
P^L, Q^L	Active power and reactive power flow on the transmission line (p.u.)
P^R, Q^F	Active power of the RES and reactive power of the shunt FACT (p.u.)
P^u, Q^u	Uncertain variable of active and reactive loads (p.u.)
$\overline{P}^u$	Uncertain variable of the maximum active power of the RES (p.u.)
V, θ	Voltage magnitude in p.u. and its angle in rad
x, w, v	Binary variables showing the presence, start-up, and shut-down status of the CGU

The associate editor coordinating the review of this manuscript and approving it for publication was Emilio Barocio.

CONSTANTS

A^R, A^G, A^D, A^F, A^L	Incidence matrices of buses and the RES, buses and the CGU, buses and the load, buses and the shunt FACT, and buses and the transmission line considering the current flow direction.
B^L, G^L	Susceptance and conductance of the transmission line (p.u.)
$MinUp$, $MinDw$	Minimum up and down times of CGU (h)
n_t, n_l, n_r	The number of simulation hours, the number of load buses, and the number of RESs
P^D, Q^D	Active loads and reactive loads (p.u.)
$\underline{P}^G$, $\overline{P}^G$	Minimum and maximum active power of the CGU (p.u.)
$\overline{P}^R$	Maximum active power of the RES (p.u.)
$\underline{Q}^F$, $\overline{Q}^F$	Minimum and maximum reactive power of the shunt FACT (p.u.)
$\underline{Q}^G$, $\overline{Q}^G$	Minimum and maximum reactive power of the CGU (p.u.)
R^D	Reserve requirement (p.u.)
$\overline{R}^G$	Maximum reserve of the CGU (p.u.)
RU, RD	Up and down ramp rates (p.u.)
$\overline{S}^L$	Maximum capacity of the transmission line (p.u.)
SU, SD	Start-up cost and shut-down cost (p.u.)
$\underline{V}$, $\overline{V}$	Minimum and maximum value of voltage (p.u)
α, β, γ	Fuel cost function coefficients of CGU in ($), ($/MWh), and ($/MWh^2), respectively.

I. INTRODUCTION

A. MOTIVATION

The security-constrained unit commitment (SCUC) is a challenging problem in power systems, which determines the commitment statuses and dispatch levels of conventional generation units (CGUs) and other generation resources to provide electricity to meet the forecasted load for a short-term interval, such as 24 hours [1], [2]. Traditionally, the problem was based on the minimum fuel cost of CGUs and the requirement to satisfy transmission network constraints and technical limitations. However, with the advancement of various technologies, such as energy storage systems (ESSs), renewable energy sources (RESs), and flexible AC transmission system (FACTS) devices, the SCUC problem included the optimal operation of these systems [3]. Based on their optimal energy management, ESSs and RESs reduced network losses and power demand from CGUs, which improved network security [4]. FACTS devices can also enhance network security by incorporating reactive power controls and voltage regulations [5]. The problem lies in the uncertainties of load forecast, power generation by RESs, and other challenges. As a result, probabilistic, stochastic, and robust model approaches were employed for the SCUC plan. probabilistic and stochastic programming methods need accurate information from the probability distribution function (PDF) with uncertain parameters. A significant number of scenarios must be generated to achieve reliable and optimal solutions using stochastic approaches [6]. Accurate PDF identification required statistical information in a long-term study period of one year, so obtaining the PDF was time-consuming [7]. Furthermore, studying various scenarios to solve the problem required long computational times, which was evident for large-scale networks [7]. With the advancement of robust optimization, researchers turned their attention to robust modeling of the SCUC problem. In this type of models, the optimal solution was obtained for the worst-case scenario [8]. Therefore, the optimal solution for other scenarios may be different from, and more favorable than, that in the robust model.

B. LITERATURE REVIEW

Numerous studies were carried out to model and solve the SCUC problem. A SCUC model was presented in [9] that considered the line outage distribution factor (LODF) index that investigated the N−1 contingency and developed a SCUC plan with shorter computational time. In [10], the generation unit reserve modeling was added to the SCUC problem with N–1 events to dispatch power with the consideration of wind generation uncertainty. The SCUC scheme subjected to reliability constraints considered a high number of transmission lines based on DC power flow (DC-PF) model, and achieved shorter computational time [11]. The SCUC modeling with a battery storage device was described in [12], in which load uncertainty modeling was based on information gap decision theory (IGDT). The uncertainty in the power generation of wind farms reduced the flexibility of the power system. Therefore, a demand response program (DRP) used in [13] improved the flexibility of the transmission network following the SCUC problem model. Robust optimization was employed to model the uncertainties in the electrical and gas systems. The robust modeling of the SCUC was presented in [14], where they obtained an optimal robust solution in the worst-case scenario for the uncertainties of the network's equipment availability. In [15], researchers modeled the reliability-constrained SCUC scheme with electric vehicles (EVs) in parking lots and the DRP, where the modeling of load and EV uncertainties were addressed by a stochastic modeling approach. References [9]–[15] used the DC-PF model in the SCUC scheme achieved shorter computational time. In DC-PF model, due to the neglect of reactive power, voltage drop, and power losses, the computational errors were expected to be non-trivial. A SCUC model was presented in accordance with AC power flow (AC-PF) in [16]–[18] that addressed this issue. The AC-SCUC modeling was described in [16]. It explored the flexibility of the power system in the presence of wind farms, controlled the structure of the transmission network that used a linearized AC-PF, and achieved

TABLE 1. Taxonomy of recent research works.

Ref	SCUC based on power flow of		Uncertainty model	Problem model	Using FACTS device
	AC	DC			
[9]	No	Yes	Stochastic	DC-PF-based MILP	No
[10]	No	Yes	Stochastic	DC-PF-based MILP	No
[11]	No	Yes	Stochastic	DC-PF-based MILP	No
[12]	No	Yes	IGDT	DC-PF-based MILP	No
[13]	No	Yes	ARO	DC-PF-based MILP	No
[14]	No	Yes	ARO	DC-PF-based MILP	No
[15]	No	Yes	Stochastic	DC-PF-based MILP	No
[16]	Yes	No	Stochastic	AC-PF-based MILP	No
[17]	Yes	No	Stochastic	AC-PF-based MILP	Yes
[18]	Yes	No	Stochastic	AC-PF-based MINLP	No
Proposed model	**Yes**	**No**	**EA-ARO**	**AC-PF-based MINLP**	**Yes**

low computational time. The linearized AC-SCUC scheme was also formulated in [17], and it considered the models of FACTS devices and energy storage devices. In [18], the evolutionary algorithm was utilized to solve the AC-SCUC problem, which used a combination of the genetic algorithm (GA) and the particle swarm optimization (PSO) algorithm.

C. RESEARCH GAPS AND CONTRIBUTIONS

Table 1 summarizes the literature review. Based on the reviewed literature, the identified main research gaps were as follows:

- Researchers in [9]–[15] considered the DC-SCUC model and evaluated the operation and security objectives of the power system that posed three major problems: first, because reactive power and voltage was ignored, DC-SCUC model did not investigate the negative effects of increased voltage deviation caused by active load and reactive load on operation and security of the system. Second, DC-SCUC model was unable to replicate the operation and planning of FACTS devices, and these elements had the capability to improve the technical and economic indices of the power system. The third problem referred to the significant inaccuracies when compared to the exact SCUC model with AC-PF. The errors in network losses, reactive power flows, and bus voltage magnitudes can be considerable.
- In [16]–[18], the AC-SCUC model was studied. In [18], traditional evolutionary algorithms (EA), such as PSO and GA, was used. The optimal solution to the problem was obtained using algorithms that require high number of iterations for convergence. Therefore the computational time was high. Most research studies presented the AC-SCUC model on small-scale networks. Studies such as [16], [17], expressed the SCUC model based on linearized AC-PF. Although the computational time improved with this method, it yielded a significant computational error of approximately 2.5 to 3% for active and reactive powers, and an error of more than 10% for network losses.
- In the robust modeling of the SCUC problem, research on adaptive robust optimization (ARO) was proposed, and in some studies, the IGDT approach was proposed. These techniques can be used to model the problem with mixed-integer linear programming (MILP) and linear programming (LP) formulations by exploiting the duality theory. Furthermore, in the MILP model, if integer variables depend on uncertain parameters, the modeling the ARO problem becomes more complicated. However, based on the aforementioned first and second research gaps, a significant computational error was observed for SCUC problem. Additionally, the implementations of some elements in the linear SCUC model were not applicable based on DC-PF.

To address the first research gap, the AC-SCUC problem was expressed in the presence of RESs and shunt FACTS devices. In the deterministic model of the proposed scheme, minimizing the fuel, starting up, and shutting down costs of the CGUs were considered as objective functions. The problem also included AC-PF constraints, transmission network technical constraints, CGU operation models, spinning reserve formulations, as well as operational constraints associated with RESs and shunt FACTS devices. This problem had mixed integer non-linear programming (MINLP) frameworks, with binary (continuous) variables that were independent (dependent) for the uncertain parameters. The uncertain parameters in this problem were the forecasted load and active power output of RESs, for which the robust optimization was employed. In this paper, in consideration of the third research gap, the evolutionary algorithm-based ARO (EA-ARO) were used to model the uncertainties. In this method, a bi-level model that did not require the use of duality theory or linearization of equations for the robust AC-SCUC problem was expressed, and its optimal solution was obtained by the EA. To address the second research gap, this paper presented a hybrid evolutionary algorithm of grey wolf optimizer (GWO) and teaching-learning-based optimization (TLBO) that achieved the optimal solution. The decision variables in the proposed algorithm were updated in three phases/processes: teacher, student, and GWO process. The number of updated phases was more than one, while non-hybrid EA such as PSO, GA, and GWO used one or two updated processes. Therefore, it was expected that the optimal solution obtained from the hybrid TLBO and GWO algorithms had a low standard deviation in the final results and low computational time with respect to non-hybrid EA. Contributions of this work include:

- Modeling of the AC-SCUC problem based on accurate nonlinear power flow in the presence of shunt FACTS devices and RESs generation in the power systems.

- Modeling of uncertainties in the load forecast and active power generation of RESs in the AC-SCUC problem using adaptive robust optimization based on the evolutionary algorithm.
- Using the hybrid TLBO and GWO algorithms to obtain a reliable optimal solution, in a comparatively low computation time, with low standard deviation.

D. PAPER ORGANIZATION

The rest of the paper was organized as follows: Section II formulated the AC-SCUC plan and considered RESs and shunt FACTS devices. Section III introduced the robust model of the AC-SCUC based on EA-ARO and described its solution method. Finally, Sections IV and V presented numerical results and conclusions, respectively.

II. THE AC-SCUC FORMULATION

This section presented the AC-SCUC problem model with transmission network and the presence of RESs and shunt FACTS. This problem minimizes the operating cost of CGUs, including fuel, start-up, and shutdown costs, while it is constrained to AC-OPF equations, CGU scheduling, and operation of RES and shunt FACTS. Therefore, the problem model was formulated as follows:

$$\min \text{Cost} = \sum_{g\in\Upsilon_G}\sum_{t\in\Upsilon_T}\left\{\begin{array}{l}\left(\alpha_g x_{g,t}+\beta_g P^G_{g,t}+\gamma_g\left(P^G_{g,t}\right)^2\right)\\ +SU_g w_{g,t}+SD_g v_{g,t}\end{array}\right\} \tag{1}$$

Subject to :

$$\sum_{\kappa\in\Upsilon_R} A^R_{\kappa,n}P^R_{\kappa,t}+\sum_{g\in\Upsilon_G} A^G_{g,n}P^G_{g,t} - \sum_{j\in\Upsilon_N} A^L_{n,j}P^L_{n,j,t}=\sum_{l\in\Upsilon_L} A^D_{l,n}P^D_{l,t} \quad \forall n,t \tag{2}$$

$$\sum_{f\in\Upsilon_F} A^F_{f,n}Q^F_{f,t}+\sum_{g\in\Upsilon_G} A^G_{g,n}Q^G_{g,t}-\sum_{j\in\Upsilon_N} A^L_{n,j}Q^L_{n,j,t} = \sum_{l\in\Upsilon_L} A^D_{l,n}Q^D_{l,t} \quad \forall n,t \tag{3}$$

$$P^L_{n,j,t}=G^L_{n,j}\left(V_{n,t}\right)^2-V_{n,t}V_{j,t}\left\{\begin{array}{l}G^L_{n,j}\cos\left(\theta_{n,t}-\theta_{j,t}\right)\\ +B^L_{n,j}\sin\left(\theta_{n,t}-\theta_{j,t}\right)\end{array}\right\} \quad \forall n,j,t \tag{4}$$

$$Q^L_{n,j,t}=-B^L_{n,j}\left(V_{n,t}\right)^2 + V_{n,t}V_{j,t}\left\{\begin{array}{l}B^L_{n,j}\cos\left(\theta_{n,t}-\theta_{j,t}\right)\\ -G^L_{n,j}\sin\left(\theta_{n,t}-\theta_{j,t}\right)\end{array}\right\} \quad \forall n,j,t \tag{5}$$

$$\sqrt{\left(P^L_{n,j,t}\right)^2+\left(Q^L_{n,j,t}\right)^2}\le \overline{S}^L_{n,j} \quad \forall n,j,t \tag{6}$$

$$\underline{V}\le V_{n,t}\le \overline{V} \quad \forall n,t \tag{7}$$

$$x_{g,t}-x_{g,t-1}\le w_{g,t} \quad \forall g,t \tag{8}$$

$$x_{g,t-1}-x_{g,t}\le v_{g,t} \quad \forall g,t \tag{9}$$

$$\tau\in\left[t+1,\min\left(t+MinUp_g-1,n_t\right)\right] \tag{10}$$

$$x_{g,t-1}-x_{g,t}\le 1-x_{g,\tau} \quad \forall g,t\ge 2,$$

$$\tau\in\left[t+1,\min\left(t+MinDw_g-1,n_t\right)\right] \tag{11}$$

$$-RD_g x_{g,t}\le P^G_{g,t}-P^G_{g,t-1}\le RU_g x_{g,t} \quad \forall g,t \tag{12}$$

$$\underline{P}^G_g x_{g,t}\le P^G_{g,t}\le \overline{P}^G_g x_{g,t} \quad \forall g,t \tag{13}$$

$$\underline{Q}^G_g x_{g,t}\le Q^G_{g,t}\le \overline{Q}^G_g x_{g,t} \quad \forall g,t \tag{14}$$

$$\underline{P}^G_g x_{g,t}\le P^G_{g,t}+R^G_{g,t}\le \overline{P}^G_g x_{g,t} \quad \forall g,t \tag{15}$$

$$0\le R^G_{g,t}\le \overline{R}^G_g \quad \forall g,t \tag{16}$$

$$\sum_{g\in\Upsilon_G} R^G_{g,t}\ge R^D_t \quad \forall t \tag{17}$$

$$P^R_{\kappa,t}=\overline{P}^R_{\kappa,t} \quad \forall \kappa,t \tag{18}$$

$$\underline{Q}^F_f\le Q^F_{f,t}\le \overline{Q}^F_f \quad \forall f,t \tag{19}$$

Eq. (1) presented the objective function of the problem, which was equal to the total fuel, start-up, and shutdown of costs of CGUs [19], [20]. The AC-OPF constraints of the transmission network in the presence of CGUs, RESs, and shunt FACTS were given in Equations (2) to (7) [21]–[23]; these equations corresponded to the balance of active power, reactive power, active power and reactive flow through the transmission line, capacity limit of the transmission line, and voltage limit [24]–[27] of the network bus, respectively [28]. The CGU scheduling constraints were formulated in Equations (8) to (17) [21], [28]. Thus, constraints (8) and (9) represented the logical limits for determining the start-up and shutdown status of the CGU [19], [20]. Equations (10) and (11) provided the minimum up time and minimum down time limitations for a CGU, respectively [20]. According to (10), if a CGU was started, it must operate for a given minimum timeframe [20]. Moreover, according to (11), if the CGU was shutdown, it had to be connected to the network after a minimum time elapsed [19]. The limitations of the ramp-up (RU) and ramp-down (RD) rates were given in (12) [20]. According to this constraint, the hourly increase/decrease in the CGU active power was due to the mechanical pressure limit on the generator shaft and could not exceed the RU/RD [19]. Formulae corresponding to the CGU capability curve were presented in (13) and (14), that indicated the permitted range of active power and reactive power changes in the CGU, respectively [28]. The reserve power of CGUs could be calculated from (15), which was limited by (16). The reserve power of all CGUs, as in (17), must be greater than the reserve requirement for the network [29], [30]. Finally, the RES and shunt FACTS operating equations appeared in (18) and (19), respectively. Generally, RESs were part of non-dispatchable distributed generation (DG). RESs had zero operating costs; thus, according to (18), RESs generated the maximum active power proportional to the available primary energy [28]. According to the IEEE-1547 standard [31], only the power generation capability of the RESs was considered in this paper. Moreover, the capability of shunt FACTS devices in the transmission network was investigated, where

these devices could be modeled as sources to change their reactive power in the ideal state, as given in (19) [32].

III. PROPOSED EA-ARO MODEL FOR SOLVING AC-SCUC PROBLEM

In the presented model formulations (1)-(19), active loads, reactive loads, and maximum power generation limit of RESs were treated as uncertain parameters. Therefore, probabilistic, stochastic, and robust optimization approaches can be used to model these parameters. The probabilistic and stochastic programming approaches required accurate PDFs of the involved uncertainties, and a large number of scenarios to obtain a guaranteed solution, that increased the computational times [7]. In contrast, the robust optimization approaches focused on the worst-case scenario, and consequently the computational time was less than the stochastic approaches' times. Also, the optimal solution in the other scenarios had more favorable conditions with respect to robust optimization results [6], [8].

In this paper, the EA-ARO method was used to obtain the optimal robust solution in the worst-case scenario. In many studies, such as [6], [14], [19], the ARO technique was used. However, ARO and other robust optimization methods, such as the boundary uncertainty-based robust optimization (BURO) model [33], were applicable to linear optimization models. Due to the use of AC power flow equations, the planning and operation problems in the power system were in the form of MINLP or nonlinear programming (NLP). These models need to be converted to a MILP or LP model, so that the ARO method and other robust optimization techniques could be used. This approach generally leads to two issues as follows:

- Most linear models for power system problems are based on DC power flow. In this model, reactive power, voltage drop, and network losses were set to zero. Therefore, the model was not suitable for problems that required analysis of the operation of reactive power devices in the power system. For network expansion planning problems, newly installed equipment was based on the growth of active load only. However, increase in load may be related to the increase of both the active and reactive loads, which may lead to issues in network expansion [21], [28].
- In previous studies, a linearized AC power flow was utilized. This had the potential to yield improved modeling accuracy compared to the DC power flow method. However, the resulting inaccuracy may still be significant for some power system operational variables, such as losses and reactive power levels [16], [17].

To eliminate the inaccuracy from power flow model simplifications, use of the practical model for power system problems was desired. Therefore, the EA-ARO technique could be applied as NLP and MINLP to these problems. The ARO method can be implemented with NLP problems; but in these problems, the requirements of the complementarity (equilibrium) constraints and duality gap complicated the problem-solving [6]. The following section described the process of the proposed technique.

A. MODELING OF UNCERTAINTIES BASED ON THE EA-ARO TECHNIQUE

The modeling process of the EA-ARO technique was the same as the ARO method. In this method, the first step was to determine the matrix of uncertain parameters, which is expressed for the problem (1) to (19) by considering P^D, Q^D, and $\overline{P}^R$ as uncertain parameters given as (20).

$$\overline{u} = \begin{bmatrix} P^D \\ Q^D \\ \overline{P}^R \end{bmatrix} \tag{20}$$

where, $\overline{u}$ denotes the predicted value of the uncertain parameters. The actual value of an uncertain parameter is unknown, therefore it was considered as an uncertain variable [19], in which case the uncertainty matrix (u) is written as:

$$u = \begin{bmatrix} P^u \\ Q^u \\ \overline{P}^u \end{bmatrix} \tag{21}$$

In (21), the number of columns in the matrix u is the number of simulation hours n_t, and the number of rows is $2 \times n_l + n_r$. The terms n_r and n_l represent the number of RESs and loads, respectively. The set of uncertainties for the ith row of the matrix u is defined as follows [34]:

$$U_i = \left\{ \begin{array}{l} u_i \in R^{n_t} : \dfrac{1}{n_t} \displaystyle\sum_{t \in \Upsilon_T} \dfrac{\left| u_{i,t} - \overline{u}_{i,t} \right|}{\tilde{u}_{i,t}} \leq \Delta_i, \\ \forall u_{i,t} \in \left[\overline{u}_{i,t} - \tilde{u}_{i,t}, \overline{u}_{i,t} + \tilde{u}_{i,t} \right] \end{array} \right\} \\ \forall i \in \bigcup (\Upsilon_L, \Upsilon_L, \Upsilon_R) \tag{22}$$

where, $\tilde{u}$ shows the uncertainty deviation for the variable u. The symbol Δ refers to the *uncertainty budget* that varied between zero and one. If it is zero, then the correct value of the variable u will be equal to its predicted value $\overline{u}$, which indicated a deterministic problem model. In robust modeling, the value of Δ is greater than zero, and $\left[\overline{u} - \tilde{u}, \overline{u} + \tilde{u}\right]$ represented the range of changes of the uncertain variable. The robust model solution was optimal only in the worst-case scenario, and this scenario was obtained from the U set. The optimal robust solution and the worst-case scenario were determined simultaneously with the ARO and/or the EA-ARO technique [34]. To better understand this, the assumed deterministic problem model is as follows:

$$\min \ f_1(z) + f_2(y) \tag{23}$$

$$\text{Subject to: } g(z) \leq 0 \tag{24}$$

$$h(z, y) \leq 0 \tag{25}$$

$$k_1(y) \leq 0 \tag{26}$$

$$k_2(y) = 0 \tag{27}$$

$$k_3(y) = \overline{u} \tag{28}$$

In the above problem, z and y are the problem variables, it was assumed that the value of the variable z is independent of the value of the uncertain parameter ($\overline{u}$), known as *here*

and now decisions [7]. The opposite is true for variable y, which was referred to as *wait and see* decisions [7]. In the proposed AC-SCUC problem, variable z is the vector of the binary variable $[x\ w\ v]^{\mathrm{T}}$, and y is the vector of the continuous variables $[P^G\ Q^G\ P^L\ Q^L\ P^R\ Q^F\ V\ \theta\ R^G]^{\mathrm{T}}$. The function f_1 was the sum of the costs of no-load $\alpha_g x_{g,t}$, start-up $SU_g w_{g,t}$, and shutdown $SD_g v_{g,t}$ of all the CGUs presented in (1), and the other terms of (1) are expressed in function f_2. Constraint (24) refers to logical Eq. (8) to (11) in the AC-SCUC problem, and constraints (12)-(15) are modeled in (25). Additionally, the constraint (26) refers to the Eqs. (6), (7), (16), (17) and (19), constraint (27) includes Eqs. (4)-(5), and constraint (28) contains Eqs. (2)-(5) and (18) in the AC-SCUC problem.

As mentioned earlier, robust optimization simultaneously determined the values of an uncertain variable, u, and the problem variables, z and y, in the worst-case scenario. Therefore, based on [19], the robust model for the problem (23)-(28) is:

$$min_{z,y}\ (f_1(z) + max_u f_2(y(u))) \tag{29}$$

Subject to: constraint (24), constraints (25)-(28) using

$$y(u) \text{ in substitution for } y, \text{ and } u \text{ for } \overline{u} \tag{30}$$

$$u \in \bigcup_{i \in \bigcup(\Upsilon_L, \Upsilon_L, \Upsilon_R)} U_i \tag{31}$$

The problem described by (23)-(28) had the expression *min* to determine the optimal value of the variables z and y; because of that, the worst-case scenario determining the value of u adopted the expression *max* in the objective function of the robust problem (29). As the variable y was dependent on the uncertain variable u, the expression *max* was used only for the function f_2. The constraints of the robust problem in (30) were equal to the constraints of the deterministic problem, that is (24)-(28), substituting $y(u)$ for y, and u for $\overline{u}$. The constraint (31) referred to the range of change of the uncertain variables. To achieve an optimal solution, the problem generated by (29)-(31) was modeled based on [24] as follows:

$$\min_z f_1(z) + \left(\max_{u \in U} \min_{y(z,u) \in \Upsilon(z,y)} f_2(y(z,u))\right) \tag{32}$$

Subject to: Constraint (24) (33)

Problem (32)-(33) refers to a bi-level problem, where the first term of the objective function (32) is $\min_z f_1(z)$, and the constraint (24) or (33) referred to its upper-level model. Moreover, the second term of the objective function was related to the lower-level model. The value of the lower-level problem variable, y, generally depended on the value of the upper-level problem variable, z, so the expression $y(z, u)$ is used in the second term of the objective function (32). The constraints of the lower-level problem were equal to the sets U and $\Upsilon(z, u)$, where the feasibility region of $\Upsilon(z, u)$ according to model (29)-(31) would be:

$$\Upsilon(z,u) = \left\{ \begin{matrix} y | h(z, y(z,u)) \le 0,\ k_1(y(z,u)) \le 0, \\ k_2(y(z,u)) = 0,\ k_3(y(z,u)) = u \end{matrix} \right\} \tag{34}$$

B. SOLUTION PROCEDURE OF THE EA-ARO ALGORITHM

Problem (32)-(33) has a nonlinear bi-level optimization framework. In this section, the hybrid evolutionary algorithms of GWO [35] and TLBO [36] was used to achieve a reliable optimal solution. The decision variables in the proposed hybrid evolutionary algorithm were updated in two processes, namely the TLBO and GWO, it was expected for this algorithm to achieve the optimal and reliable solution in the shortest computation time. Another advantage of this algorithm was that the adjustment parameter did not require definitions [35], [36]. To present the solution procedure for the problem (32)-(33), in accordance with the proposed algorithm, the first step was to determine the decision and dependent variables. In the proposed method, the values of the decision variables were determined by the hybrid GWO and TLBO algorithm, and the dependent variables were calculated according to the values of decision variables and equality constraints used numerical solution methods, such as Newton-Raphson. In the upper-level model of the problem (32)-(33) and the AC-SCUC, z—the vector $[x\ w\ v]^{\mathrm{T}}$—is the decision variable. In the lower-level model of the problem, the uncertain variable u—the vector $[P^u\ Q^u\ \overline{P}^u]^{\mathrm{T}}$ in the robust model of the AC-SCUC—is the decision variable. In this problem, y_d and y_i are also used as decision and dependent variables in the function f_2, where the vectors $[P^G\ Q^G\ Q^F\ R^G]^{\mathrm{T}}$ and $[P^L\ Q^L\ P^R\ V\ \theta]^{\mathrm{T}}$ are y_d and y_i in the AC-SCUC problem, respectively. Also, in this problem, the fitness function (FF) was proportional to (32) and the AC-SCUC problem model (1)-(19) was written as (35):

$$\begin{aligned}
&min_{x,w,v} \\
&\overbrace{\sum_{g\in\Upsilon_G}\sum_{\in\Upsilon_T}\{\alpha_g x_{g,t} + SU_g w_{g,t} + SD_g v_{g,t}\}}^{f_1} \\
&+ \sum_{g\in\Upsilon_G}\sum_{t\in\Upsilon_T} \mu^{su}_{g,t} max\left(0, x_{g,t} - x_{g,t-1} - w_{g,t}\right) \\
&+ \mu^{sd}_{g,t} max\left(0, x_{g,t-1} - x_{g,t} - v_{g,t}\right) \\
&+ \sum_{g\in\Upsilon_G}\sum_{\substack{t\in\Upsilon_T \\ t\neq 1}} \sum_{\tau=t+1}^{min(t+MinUp_g-1, n_T)} \mu^{MinUp}_{g,\tau} \\
&\times max\left(0, x_{g,t} - x_{g,t-1} - x_{g,\tau}\right) \\
&+ \sum_{g\in\Upsilon_G}\sum_{\substack{t\in\Upsilon_T \\ t\neq 1}} \sum_{\tau=t+1}^{min(t+MinDw_g-1, n_T)} \mu^{MinDw}_{g,\tau} \\
&\times max\left(0, x_{g,t-1} - x_{g,t} - 1 + x_{g,\tau}\right) \\
&+ max_{P^u, Q^u, \overline{p}^u} min_{P^G, Q^G, R^G, Q^F, P^R, P^L, Q^L, V, \theta} \\
&\overbrace{\sum_{g\in\Upsilon_G}\sum_{t\in\Upsilon_T}\left\{\beta_g P^G_{g,t} + \gamma_g\left(P^G_{g,t}\right)^2\right\}}^{f_2} \\
&+ \sum_{g\in\Upsilon_G}\sum_{t\in\Upsilon_T} \overline{u}^{rr}_{g,t} max\left(0, P^G_{g,t} - P^G_{g,t-1} - RU_g x_{g,t}\right) \\
&+ \sum_{g\in\Upsilon_G}\sum_{t\in\Upsilon_T} \underline{\mu}^{rr}_{g,t} max\left(0, -RD_g x_{g,t} - P^G_{g,t} + P^G_{g,t-1}\right)
\end{aligned}$$

$$+\sum_{g\in\Upsilon_G}\sum_{t\in\Upsilon_T}\overline{u}^{re}_{g,t}max\left(0,P^G_{g,t}+R^G_{g,t}-\overline{p}^G_g x_{g,t}\right)$$
$$+\sum_{g\in\Upsilon_G}\sum_{t\in\Upsilon_T}\underline{\mu}^{re}_{g,t}max\left(0,\underline{P}^G_g x_{g,t}-P^G_{g,t}-R^G_{g,t}\right)$$
$$+\sum_{t\in\Upsilon_T}\mu^{rd}_t max\left(0,R^D_t-\sum_{g\in\Upsilon_G}R^G_{g,t}\right)$$
$$+\sum_{n,j\in\Upsilon_N}\sum_{t\in\Upsilon_T}\mu^{sl}_{n,j,t}max\left(0,\sqrt{\left(P^L_{n,j,t}\right)^2+\left(Q^L_{n,j,t}\right)^2}-\overline{S}^L_{n,j}\right)$$
$$+\sum_{n\in\Upsilon_N}\sum_{t\in\Upsilon_T}\overline{u}^{v}_{n,t}max\left(0,V_{n,t}-\overline{V}\right)+\underline{\mu}^{v}_{n,t}max\left(0,\underline{V}-V_{n,t}\right) \quad (35)$$

In equation (35), the constraints (6)-(12), (15), and (17) were added as a penalty function to the objective function of (32) [37]. The penalty function for a constraint of $a \leq b$ has the relation μ.max(0, a - b) based on [37], where μ represents the price of the penalty and is considered the decision variable. Constraints (8)-(11) are related to the upper-level problem, so their penalty functions were added to the f_1 function. Other constraints are part of the lower-level problem constraints, so their penalty functions were added to the f_2 function. In addition, in these conditions, the decision-making (DM) variables were in the form of (36).

$$DM=\left[x\ w\ v\ P^u\ Q^u\ \overline{P}^u\ P^G\ Q^G\ Q^F\ R^G\ \mu\right]^T \quad (36)$$

The problem was solved using the following steps:

- *Step* 1 (*Initialization step*): This process determined N random values for the DM vector, where the random values x, w, v, P^u, Q^u, $\overline{P}^u$, P^G, Q^G, R^G, Q^F, and μ respectively corresponded to the sets {0, 1}, {0, 1}, {0, 1}, U, U, U (13), (14), (16), (19) and the interval [0, $+\infty$). Then the dependent variables were calculated for N random values of the DM vector. The value of P^R, proportional to (18), is $\overline{P}^u$. The values of variables P^L, Q^L, V, and θ were also calculated using AC-PF equations, i.e., constraints (2)-(5), based on Newton-Raphson numerical solution method. Lastly, the fitness function, or FF, of the proposed problem were calculated using (35).
- *Step* 2 (*Updating decision variables*): In this section, N values of the DM vector were updated using the hybrid GWO and TLBO algorithm, first the teacher phase and then the student phase of the TLBO algorithm were implemented; thus, the GWO algorithm updated the decision variables. Then, similar to the first step, the values of dependent variables and the fitness function were calculated. If the value of the FF was more optimal than the previous step, then the new values of decision variables were equal to the values obtained in this step. Otherwise, those were equal to the values of decision variables in the previous step.
- *Step* 3 (*Checking the convergence*): It was assumed that the optimal solution was available after maximum iterations ($iter_{max}$). Hence, the second step was repeated as much as $iter_{max}$.

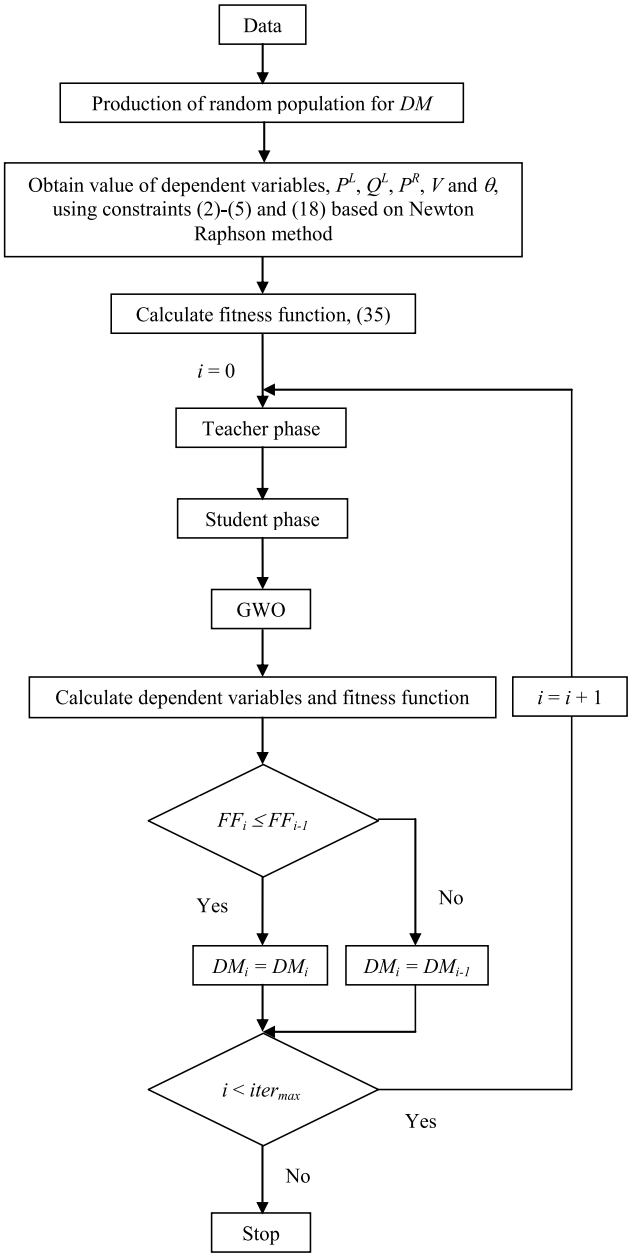

FIGURE 1. Flowchart of hybrid algorithm of GWO and TLBO for the proposed AC-SCUC model.

In the end, the flowchart of the hybrid GWO and TLBO algorithm for the robust AC-SCUC problem (32)-(33) is shown in Fig. 1.

IV. NUMERICAL RESULTS AND DISCUSSION

The numerical results of the proposed AC-SCUC problem applied to the modified IEEE 6-bus and IEEE 118-bus networks were described in this section. In the EA-ARO, the term $\tilde{u}$ is considered to be equal to $r.\overline{u}$, where r represents

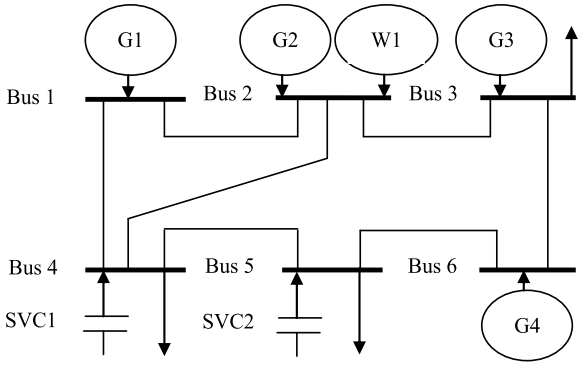

FIGURE 2. Single-line diagram of modified IEEE 6-bus network [38].

TABLE 2. Specifications of generation units and shunt FACTS devices [32], [38].

Network component	G1	G2	G3	
Min (P) (MW)	1	1	0.5	
Max (P) (MW)	10	10	6	
Min (Q) (MVAr)	-3	-3	-1.5	
Max (Q) (MVAr)	6	6	3	
RU/ RD (MW)	4	4	2	
Max (R) (MW)	3	3	1.5	
SU/ SD ($)	200/ 200	200/ 200	150/ 150	
$MinUp$/ $MinDw$ (hour)	3/ 3	3/ 3	5/ 5	
α ($)/ β ($/MWh)/ γ ($/MWh^2)	500/25/0.003	500/25/0.003	600/35/0.004	
Network component	G4	W1	SVC1	SVC2
Min (P) (MW)	0.5	0	-	-
Max (P) (MW)	6	10	-	-
Min (Q) (MVAr)	-1.5	-	-1	-1
Max (Q) (MVAr)	3	-	5	5
RU/ RD (MW)	2	-	-	-
Max (R) (MW)	1.5	-	-	-
SU/ SD ($)	150/ 150	-	-	-
$MinUp$/ $MinDw$ (hour)	5/ 5	-	-	-
α ($)/ β ($/MWh)/ γ ($/MWh^2)	620/37/0.004	-	-	-

the "*uncertainty level*". Also, the population size (N) and the maximum iterations ($iter_{max}$) for the hybrid GWO and TLBO (GWO + TLBO) algorithm were 50 and 3000, respectively.

A. THE MODIFIED IEEE 6-BUS NETWORK

1) DATA

Modified IEEE 6-bus networks [28] in the presence of CGUs (G1 to G4), RESs (wind farms) (W1), shunt FACTS devices with static var compensators (SVC1 and SVC2) are presented in Fig. 2. This network had a base power and voltage of 100 MW and 230 kV, with the allowed voltage range of [0.95, 1.05] p.u. [21]. The specifications of transmission lines were extracted from [28], the data for generation units and shunt FACTS devices are listed in Table 2 [28], [32], [38]. The term $\overline{P}^R$ is the product of the capacity of wind farms and the daily power rate curve. The capacities of wind farms are presented in Table 2, and the daily power rate curve of this renewable source is plotted in Fig. 3(a). The network had a peak load of 25 MW with a power factor of 0.9, of which 40%, 30%, and 30% were respectively consumed in buses 3, 4, and 5. Also, the amount of load during other hours was obtained from the product of the load factor's daily curve and the peak load, which is plotted in Fig. 3(a). Finally, it was assumed that each bus with a generation unit had a daily reserve demand curve (R^D), as shown in Fig. 3(b) [39].

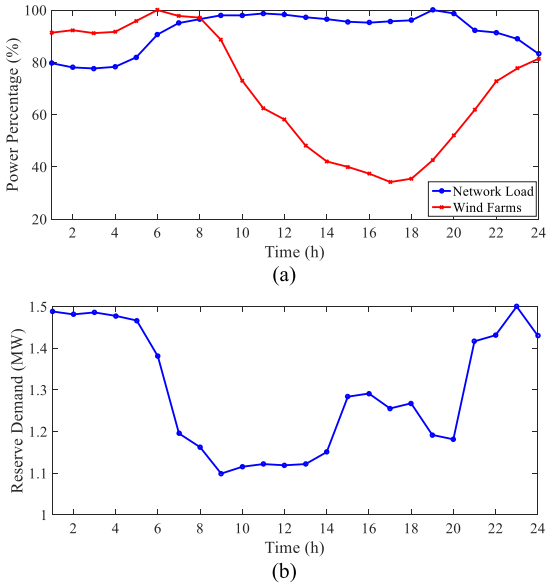

FIGURE 3. Daily curves of a) Load factor and wind farm power rate [39], and b) reserve demand in a bus with a generation unit [39].

TABLE 3. Convergence results of different solution algorithms for an uncertainty budget of 100% for modified IEEE 6-bus network.

Parameter	r	Algorithm				
		CSA	KHO	TLBO	GWO	GWO+TLBO
Convergence iteration	0	1289	1236	989	1007	782
	0.1	1402	1347	1056	1083	845
	0.2	1611	1553	1107	1155	903
Convergence time (sec)	0	89.3	78.9	64.2	63.5	54.2
	0.1	98.8	87.1	69.5	68.7	59.1
	0.2	107.9	95.6	74.6	73.4	63.8
Mean value of objective function ($)	0	65567	65273	64311	64477	63488
	0.1	67892	67672	66692	66812	65796
	0.2	70471	70223	68187	69291	68280
Standard deviation (%)	0	2.86	2.51	1.69	1.87	0.92
	0.1	3.98	3.36	1.86	2.11	0.93
	0.2	5.08	4.13	2.02	2.45	0.93

2) INVESTIGATING THE CAPABILITY OF THE PROPOSED ALGORITHM

In this section, the crow search algorithm (CSA) [40], krill herd optimization (KHO) [41], TLBO, GWO, and hybrid TLBO and GWO (TLBO + GWO) algorithm were considered to obtain the optimal solution of the robust AC-SCUC problem with an uncertainty budget of 100%. The results are summarized in Table 3, and the reported results in this table were the average of 10 simulations for each algorithm. The population size of 50 and the maximum number of iterations equal to 3000 were selected, and the values of regulation parameters of each algorithm were selected from [35], [36], [40], [41]. Based on Table 3, it was observed that when compared to the other algorithms mentioned in this table, the hybrid TLBO-GWO algorithm obtained the

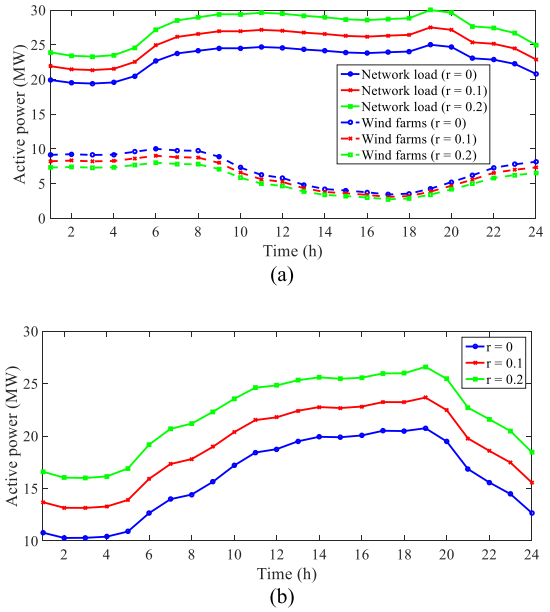

FIGURE 4. The daily active power curve of a) network load and wind farm generation, b) net power consumption for an uncertainty budget of 100%.

minimum mean of the objective function (32), i.e., \$63488 in the shortest computational time of 54.2 seconds, and the lowest number of convergence iterations of 782 for the deterministic model of the AC-SCUC problem ($r = 0$). This algorithm had a low standard deviation of 0.92%, when compared to CSA, KHO, TLBO, and GWO algorithms. Increasing the degree of uncertainty (r) also increased the mean of the objective function, the computational time or convergence time, the number of convergence iterations, and the standard deviation of the solution. This was because increased uncertainty level in worst-case scenario, based on model (32) and [6], [8], meant a reduction in the feasible region of the robust problem when compared to that of the deterministic problem. However, for different values of r, the proposed hybrid TLBO and GWO algorithm outperforms the other algorithms based on simulation results that included low standard deviation, convergence iteration, computation time, and minimum objective function, which was similar to the results from the deterministic model. It was observed that the standard deviation changes minimally with the changes in the uncertainty level; that was not the case in the CSA, KHO, TLBO, and GWO algorithms. This suggested that the proposed algorithm could find a reliable optimal solution with a low standard deviation that had a low dependence on the feasibility region and the volume of the problem. Finally, the results of this section confirmed the second research gap in Section 1 and demonstrated the third contribution provided in Section 1.

3) PERFORMANCE EVALUATION OF GENERATION UNITS AND SHUNT FACTS DEVICES

Fig. 4 illustrated the daily load curve of the network and the active power of wind farms in the robust AC-SCUC

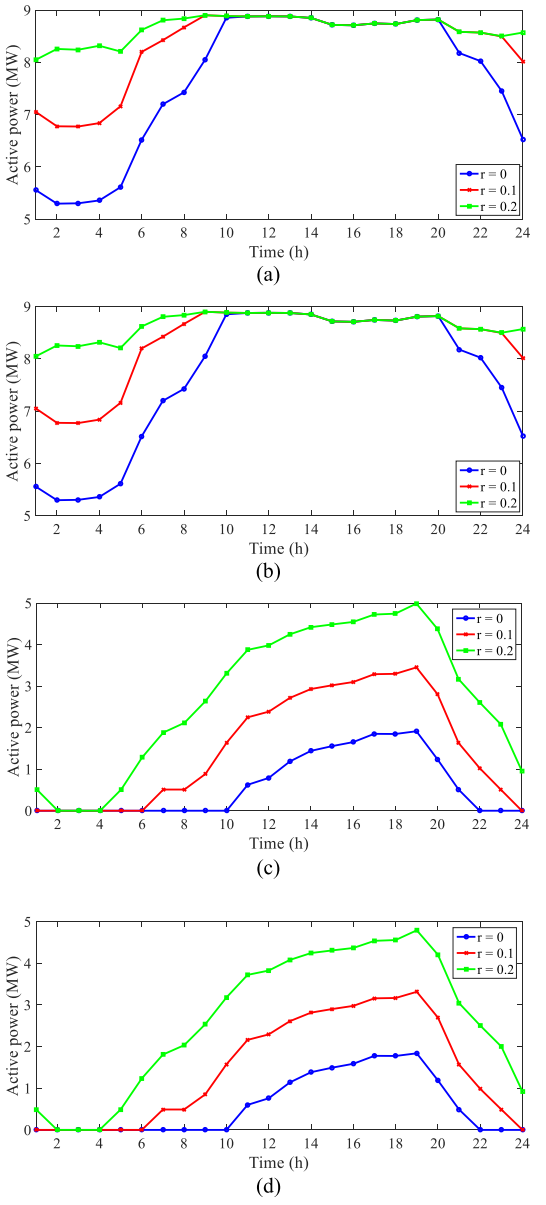

FIGURE 5. The daily active power curve of a) G1, b) G2, c) G3, and d) G4 for an uncertainty budget of 100%.

problem for an uncertainty budget of 100%. According to Fig. 4(a), the injected active power of wind farms was equal to their maximum capacity for the network, this was echoed in Fig. 3(a) and the data of Table 2 and can be attributed to zero operation costs of these resources. Following Fig. 3(a), increasing the uncertainty level to achieve the worst-case scenario and reducing the feasible region of the robust problem, when compared with the deterministic problem, ($r = 0$) increased the active load of the network and reduced the capacity of active wind farms. In Fig. 4(b), the net power demand of the network—which was equal to the difference between the load of the network and the generation power of wind farms—increased with the increase in uncertainty levels during all simulation hours. This was because the peak load of

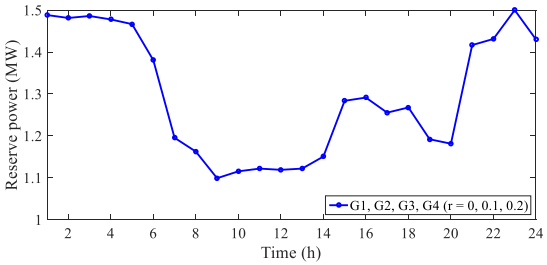

FIGURE 6. The daily reserve power curve of CGUs for an uncertainty budget of 100%.

the network (25 MW) was approximately 150% greater than the capacity of wind farms (10 MW), referring to the data in subsection 4.A.

Fig. 5 presents the daily active power curve of CGUs in the robust AC-SCUC problem for an uncertainty budget of 100%. In this figure, G1 and G2 could produce active power to supply power consumption of the network in all simulation hours because, as presented Table 2, they had a lower fuel price (α, β, γ) than other CGUs. Due to the high operation cost, G3 and G4 were not operated to supply energy during some hours, during which they had zero active power. In the robust model ($r = 0.1$ and $r = 0.2$) compared to the deterministic model ($r = 0$), G1 and G2 supplied active power that was near the difference between their capacity and the required reserve ($\overline{P}^G - R^D$) during more hours. Moreover, the number of hours with zero generation of active power by G3 and G4 in these conditions decreased compared to the case of $r = 0$, and the generation of these resources increased in the robust model compared to the deterministic model of the AC-SCUC problem. As shown in Fig. 4(b), the net load consumption increased with the increase of the uncertainty level. In addition, the daily reserve power curves of CGUs in the robust model of the proposed problems with an uncertainty budget of 100% was shown in Fig. 6. Comparing Fig. 6 with Fig. 3(b), all CGUs were procured R^D at all simulated hours and did not incur more reserves than that. Also, in Bus 2 with wind farms and G2, only G2 provided the demand reserve power for Bus 2, and wind farms did not play a role in providing reserves. Wind farms could provide energy because of their zero operating costs to minimize operating costs or their energy costs in the objective function (32).

The daily reactive power curves of CGUs and shunt FACTS devices in the robust AC-SCUC model with an uncertainty budget of 100% are shown in Fig. 7. According to Fig. 7(a), only G3 and G4 were used to supply reactive power to Bus 3 because it was desirable to operate generation resources G3 and G4, which were close to the load, to reduce network losses. Other units used their maximum capacity in supplying power and reserve, and so they had no role in supplying the network reactive loads. The peak reactive power of the network was 12.1 MVAr ($=25^{(\mathrm{MW})} \times \tan(\cos^{-1}(0.9))$), 30% of which—3.6 MVAr—appeared at Buses 4 and 5. According to Table 2, the capacity of each of the SVCs installed in these

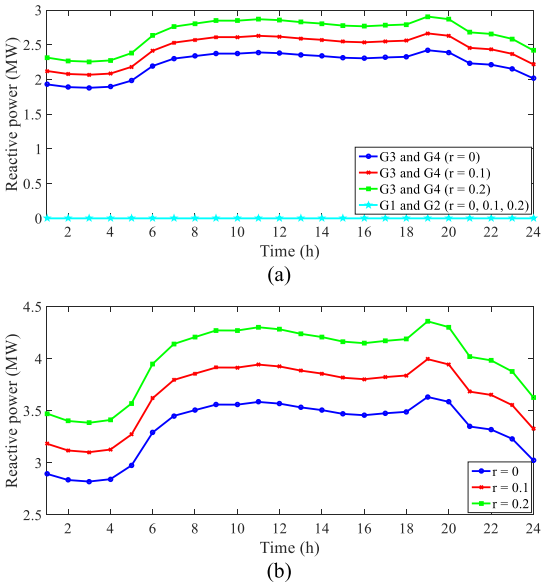

FIGURE 7. The daily reactive power curve of a) CGUs, and b) SVCs for an uncertainty budget of 100%.

TABLE 4. Economic and technical results of the robust AC-SCUC plan for an uncertainty budget of 100%.

r	0.5	0.4	0.3	0.2	0.1	0
Operation cost ($)	69523	69523	69171	68280	65796	63488
Total start up and shut down cost ($)	0	0	0	0	0	0
The robustness cost of robust model ($)	6035	6035	5683	4792	2308	0
Energy loss (MWh)	16.09	16.09	16.01	15.81	13.66	11.43
Maximum voltage deviation (p.u)	0.040	0.040	0.040	0.040	0.039	0.038

buses was equal to 5 MVAr, thus they provided all the reactive loads for the buses, as seen in Fig 7(b). Also, increased uncertainty level, outlined in Fig. 7, increased the reactive load of the network and the reactive power generation of CGUs and shunt FACTS devices were also increased. Finally, ancillary services were considered, such as setting up reactive power reserves for CGUs, that enabled them to participate in ancillary services when the commitment of a unit was not economically viable. It was expected that the cost of shutting down and restarting the unit would be reduced to zero. This was true for G3 and G4 in Figs. 5-7. This demonstrated the first contribution given in Section 1.

4) STUDY OF ECONOMIC AND TECHNICAL BENEFITS

Table 4 shows the values using economic indices (such as operation and shutdown/start-up costs and the robustness cost of robust model) and technical indices (such as energy losses and maximum voltage deviation) in the robust AC-SCUC formulation for an uncertainty budget of 100%. This table shows the increased uncertainty levels increased the operating costs of CGUs until they reached saturation point at $r = 0.4$, meaning that further increasing r did not cause changes in operating costs. Also, the cost of shutting down and restarting CGUs was always zero because, according

TABLE 5. Convergence results of different solution algorithms for an uncertainty budget of 100% for IEEE 118-bus network.

Parameter	r	Algorithm				
		CSA	KHO	TLBO	GWO	GWO+TLBO
Convergence iteration	0	2711	2659	2136	2311	1722
	0.1	2820	2761	2221	2408	1804
	0.2	2929	2870	2315	2501	1897
Convergence time (sec)	0	133.1	122.5	108.1	111.2	99.1
	0.1	144.2	131.3	114.5	119.4	104.8
	0.2	154.4	141.2	120.3	126.2	109.3
Mean value of objective function (M$)	0	33.3	33.1	32.5	32.6	31.9
	0.1	34.5	34.3	33.5	33.7	32.8
	0.2	36.1	35.9	34.9	35.0	34.3
Standard deviation (%)	0	3.93	3.62	1.98	2.09	0.93
	0.1	5.08	4.71	2.36	2.48	0.93
	0.2	6.51	5.80	2.79	2.99	0.94

to Figs. 5-7, CGUs could participate in ancillary services, such as reserve adjustment and reactive power supply, that eliminated or reduced the cost. The robustness cost of robust model referred to the difference between cost in robust ($r > 0$) and deterministic ($r = 0$) formulations. According to Table 4, increased uncertainty level (to 0.4) resulted in an increased cost to $6035. Hence, it could be said that considering forecasting error of uncertainty parameters in the proposed scheme increased the CGUs' operation cost with respect to the deterministic model, where the maximum value of this robustness cost is 6035$. Energy loss was equal to the total network losses on the operation horizon, or 24 hours, and the maximum voltage deviation can be calculated as $max(|1 - V_{n,t}|)$. Based on the results in Table 4, increasing r led to increased energy losses that reached its saturation point of 16.09 MWh at $r = 0.4$. Compared to the deterministic model of the proposed problem ($r = 0$), this value grew by about 39.8%. Increasing r also increased the maximum voltage deviation, and it reached its saturation point of 0.04 p.u. at $r = 0.2$. This rate of voltage deviation was less than its maximum allowable values of 0.05 p.u., 1-1.05, or 0.95-1. Therefore, in the worst-case, favorable operational and economic conditions can be achieved by adopting the proposed AC-SCUC plan, which demonstrated the first and second contributions given in Section 1.

B. THE IEEE 118-BUS NETWORK

The IEEE 118-bus network included 54 CGUs, 186 transmission lines, and 91 buses, the data from which were consistent with the data presented in [42]. Load characteristics, such as power factors and daily load curves were the same as the data presented in Section 4.1. Based on the results of optimal planning for wind farms in [43], this network had four wind farms with capacities of 500, 800, 200, and 500 MW that were respectively installed in buses 10, 15, 30, and 75. Their daily power rate curve was the same as in Fig. 3(a). Finally, the daily curve of the reserve demand for buses with generation units was 10 times the hourly data presented in Fig. 3(b).

The convergence results of the robust AC-SCUC optimization in the uncertainty budget of 100% obtained by CSA, KHO, TLBO, GWO, and TLBO + GWO for IEEE 118-bus network is reported in Table 5. Accordingly, TLBO + GWO could be achieved to minimize cost in the lower convergence iteration and calculation time in comparison with CSA, KHO, TLBO, and GWO. Also, it included low standard deviation in the final solution, where fluctuated uncertainty level is low, while this issue is not true for other solvers. Therefore, subsection IV-A-2, solver of TLBO + GWO, included suitable capabilities with respect to other algorithms.

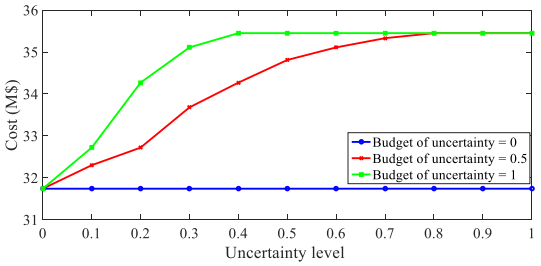

FIGURE 8. Cost curve in terms of the uncertainty level for different values of uncertainty budget.

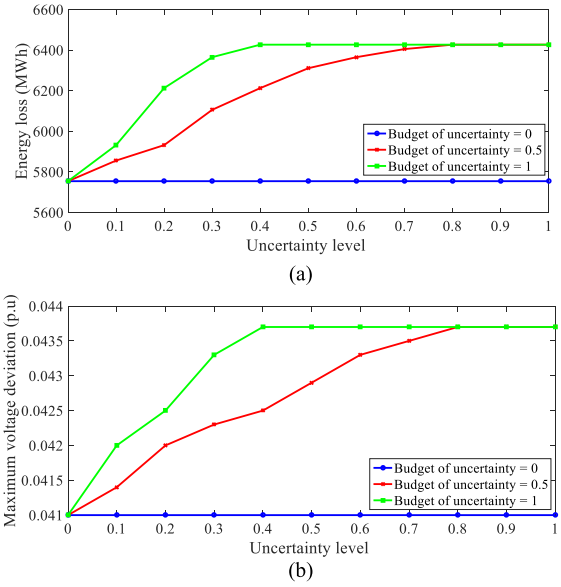

FIGURE 9. Curves of a) energy loss, and b) maximum voltage deviation in terms of the uncertainty level for different values of the uncertainty budget.

The economic results of the AC-SCUC plan for the transmission network are presented in Fig. 8, which showed the diagram of the total costs of fuel, shutdown, and restarting of CGUs in terms of the uncertainty level (r). Accordingly, in the zero-uncertainty budget for the AC-SCUC plan, increased uncertainty level did not change the cost of CGUs. According to Section 3.1, zero uncertainty budget meant a deterministic model in which the value of the uncertainty variable was equal to the predicted values of the uncertainty parameter, and the value of $\tilde{u}$ is zero. Thus, changing the value of r did not affect the value of $\tilde{u}$. Nonetheless, for other values of the uncertainty budget, increasing r increased the cost of CGUs

until it reached saturation. The saturation zone was created using the technical limitations of the network and CGUs. At higher uncertainty budget values, the saturation point was set at a lower level of uncertainty, as in Fig. 8, because the change percentage for uncertainty variables was higher when compared to the deterministic model for larger values of the uncertainty budget. The opposite was true for low values of the uncertainty budget.

Fig. 9 showed the curves of the network technical indices, such as energy losses and maximum voltage deviations, in terms of the uncertainty level for different values of the uncertainty budget based on the robust AC-SCUC plan. These curves exhibited the same trend as the cost curves presented in the Fig. 8. In the case corresponding to the zero-uncertainty budget, changes in the uncertainty level did not cause a change in the values of technical indices. Moreover, for higher values of the uncertainty budget, increasing r led increased mentioned indices until they reached the saturation point for a certain value of r.

V. CONCLUSION

This research attempted to solve the AC-SCUC problem considering the uncertainty of load forecast and RESs generation forecast in the presence of shunt FACTS devices. The objective of the proposed model was to minimize the operating costs of CGUs subject to AC power flow equations, operation constraints of RESs and shunt FACTS devices, and the operation models of CGUs. In this study, an EA-ARO technique was utilized to model the load uncertainties and the generation power uncertainties of the RESs and to achieve the optimal solution of the nonlinear AC-SCUC problem. The resultant model was solved using a GWO and TLBO hybrid algorithm. Based on the numerical results, it was observed that the hybrid GWO and TLBO algorithm achieved the most optimal and reliable solution in the least computational time with the minimum iterations to converge: the standard deviation of the final solution was approximately 0.9%, and its dependence on the feasible region and the problem complexity was very low. In addition, studies of the proposed AC-SCUC model showed low-cost CGUs were always utilized near their capacities to supply power and reserve. However, for CGUs with high fuel prices, their participation in supplying power was not economically justified for some hours. It can save the shutdown and restart costs by participating in ancillary services, such as reserve and reactive power. Finally, the proposed method provided the optimal scheduling for active power, reactive power, CGUs reserves, and reactive power of shunt FACTS. Furthermore, it yielded desired results in terms of the network operational metrics, such as energy loss and maximum voltage deviation, even in the worst-case situation. In worst-case situation, the voltage deviation was always less than its maximum limit of 0.05 p.u., and the energy loss in the worst-case situation with a high uncertainty budget and high uncertainty level was about 40% when compared to the scenario corresponding to the deterministic model.

REFERENCES

[1] F. H. Aghdam and M. T. Hagh, "Security constrained unit commitment (SCUC) formulation and its solving with modified imperialist competitive algorithm (MICA)," *J. King Saud Univ.-Eng. Sci.*, vol. 31, no. 3, pp. 253–261, Jul. 2019.
[2] S. Badakhshan, M. Ehsan, M. Shahidehpour, N. Hajibandeh, M. Shafie-Khah, and J. P. S. Catalão, "Security-constrained unit commitment with natural gas pipeline transient constraints," *IEEE Trans. Smart Grid*, vol. 11, no. 1, pp. 118–128, Jan. 2020.
[3] M. Ghaljehei, A. Ahmadian, M. A. Golkar, T. Amraee, and A. Elkamel, "Stochastic SCUC considering compressed air energy storage and wind power generation: A techno-economic approach with static voltage stability analysis," *Int. J. Electr. Power Energy Syst.*, vol. 100, pp. 489–507, Sep. 2018.
[4] P. P. Gupta, P. Jain, K. C. Sharma, and R. Bhakar, "Stochastic scheduling of compressed air energy storage in DC SCUC framework for high wind penetration," *IET Gener., Transmiss. Distrib.*, vol. 13, no. 13, pp. 2747–2760, 2019.
[5] J. Liu, Z. Xu, J. Yang, and Z. Zhang, "Modeling and analysis for global and local power flow operation rules of UPFC embedded system under typical operation conditions," *IEEE Access*, vol. 8, pp. 21728–21741, 2020.
[6] S. Pirouzi, J. Aghaei, M. A. Latify, G. R. Yousefi, and G. Mokryani, "A robust optimization approach for active and reactive power management in smart distribution networks using electric vehicles," *IEEE Syst. J.*, vol. 12, no. 3, pp. 2699–2710, Sep. 2017.
[7] A. J. Conejo, E. Castillo, R. Minguez, and R. Garcid-Bertrand, *Decomposition Techniques in Mathematical Programming*. Berlin, Germany: Springer-Verlag, 2006.
[8] A. Shahbazi, J. Aghaei, S. Pirouzi, M. Shafie-Khah, and J. P. S. Catalão, "Hybrid stochastic/robust optimization model for resilient architecture of distribution networks against extreme weather conditions," *Int. J. Electr. Power Energy Syst.*, vol. 126, Mar. 2021, Art. no. 106576.
[9] D. A. Tejada-Arango, P. Sánchez-Martín, and A. Ramos, "Security constrained unit commitment using line outage distribution factors," *IEEE Trans. Power Syst.*, vol. 33, no. 1, pp. 329–337, Jan. 2018.
[10] K. Sundar, H. Nagarajan, L. Roald, S. Misra, R. Bent, and D. Bienstock, "Chance-constrained unit commitment with N-1 security and wind uncertainty," *IEEE Trans. Control Netw. Syst.*, vol. 6, no. 3, pp. 1062–1074, Sep. 2019.
[11] A. S. Xavier, F. Qiu, F. Wang, and P. R. Thimmapuram, "Transmission constraint filtering in large-scale security-constrained unit commitment," *IEEE Trans. Power Syst.*, vol. 34, no. 3, pp. 2457–2460, May 2019.
[12] A. Ahmadi, A. E. Nezhad, and B. Hredzak, "Security-constrained unit commitment in presence of lithium-ion battery storage units using information-gap decision theory," *IEEE Trans. Ind. Informat.*, vol. 15, no. 1, pp. 148–157, Jan. 2019.
[13] H. Safipour, A. Abdollahi, M. S. Hajmohammadi, and M. I. Alizadeh, "Optimal demand response strategies to mitigate wind power variability and gas-supply uncertainty in a multi-resolution robust security constrained unit commitment," *IET Gener., Transmiss. Distrib.*, vol. 14, no. 14, pp. 2740–2750, Jul. 2020.
[14] J. Jeong and S. Park, "A robust contingency-constrained unit commitment with an N-αk security criterion," *Int. J. Electr. Power Energy Syst.*, vol. 123, Dec. 2020, Art. no. 106148.
[15] M. Rahmani, S. H. Hosseinian, and M. Abedi, "Stochastic two-stage reliability-based security constrained unit commitment in smart grid environment," *Sustain. Energy, Grids Netw.*, vol. 22, Jun. 2020, Art. no. 100348.
[16] A. Nikoobakht, M. Mardaneh, J. Aghaei, V. Guerrero-Mestre, and J. Contreras, "Flexible power system operation accommodating uncertain wind power generation using transmission topology control: An improved linearised AC SCUC model," *IET Gener., Transmiss. Distrib.*, vol. 11, no. 1, pp. 142–153, Jan. 2017.
[17] Z. Luburić and H. Pandžić, "FACTS devices and energy storage in unit commitment," *Int. J. Electr. Power Energy Syst.*, vol. 104, pp. 311–325, Jan. 2019.
[18] N. Amjady and H. Nasiri-Rad, "Security constrained unit commitment by a new adaptive hybrid stochastic search technique," *Energy Convers. Manage.*, vol. 52, no. 2, pp. 1097–1106, Feb. 2011.
[19] D. Bertsimas, E. Litvinov, X. A. Sun, J. Zhao, and T. Zheng, "Adaptive robust optimization for the security constrained unit commitment problem," *IEEE Trans. Power Syst.*, vol. 28, no. 1, pp. 52–63, Feb. 2013.
[20] S. S. Reddy, P. R. Bijwe, and A. R. Abhyankar, "Faster evolutionary algorithm based optimal power flow using incremental variables," *Int. J. Electr. Power Energy Syst.*, vol. 54, pp. 198–210, Sep. 2014.

[21] M. R. Ansari, S. Pirouzi, M. Kazemi, A. Naderipour, and M. Benbouzid, "Renewable generation and transmission expansion planning coordination with energy storage system: A flexibility point of view," *Appl. Sci.*, vol. 11, no. 8, p. 3303, Apr. 2021.

[22] S. S. Reddy, A. R. Abhyankar, and P. R. Bijwe, "Optimal day-ahead joint energy and reactive power scheduling with voltage dependent load models," in *Proc. IEEE Transp. Electrific. Conf. Expo, Asia–Pacific (ITEC Asia–Pacific)*, Jun. 2016, pp. 198–202.

[23] S. S. Reddy, B. K. Panigrahi, P. R. Bijwe, and A. R. Abhyankar, "Comparison and application of swarm intelligent techniques to optimal power flow," in *Proc. Joint Int. Conf. Power Electron., Drives Energy Syst. Power India*, Dec. 2010, pp. 1–6.

[24] M. Norouzi, J. Aghaei, S. Pirouzi, T. Niknam, and M. Lehtonen, "Flexible operation of grid-connected microgrid using ES," *IET Gener., Transmiss. Distrib.*, vol. 14, no. 2, pp. 254–264, Jan. 2020.

[25] J. Aghaei, S. A. Bozorgavari, S. Pirouzi, H. Farahmand, and M. Korpås, "Flexibility planning of distributed battery energy storage systems in smart distribution networks," *Iranian J. Sci. Technol., Trans. Electr. Eng.*, vol. 44, no. 3, pp. 1105–1121, Sep. 2020.

[26] A. Shahbazi, J. Aghaei, S. Pirouzi, T. Niknam, M. Shafie-Khah, and J. P. S. Catalão, "Effects of resilience-oriented design on distribution networks operation planning," *Electr. Power Syst. Res.*, vol. 191, Feb. 2021, Art. no. 106902.

[27] A. Dini, S. Pirouzi, M. Norouzi, and M. Lehtonen, "Hybrid stochastic/robust scheduling of the grid-connected microgrid based on the linear coordinated power management strategy," *Sustain. Energy, Grids Netw.*, vol. 24, Dec. 2020, Art. no. 100400.

[28] H. Hamidpour, J. Aghaei, S. Dehghan, S. Pirouzi, and T. Niknam, "Integrated resource expansion planning of wind integrated power systems considering demand response programmes," *IET Renew. Power Gener.*, vol. 13, no. 4, pp. 519–529, Mar. 2019.

[29] S. S. Reddy, P. R. Bijwe, and A. R. Abhyankar, "Optimal dynamic emergency reserve activation using spinning, hydro and demand-side reserves," *Frontiers Energy*, vol. 10, no. 4, pp. 409–423, Dec. 2016.

[30] S. S. Reddy, "Emergency reserve activation considering demand-side resources and battery storage in a hybrid power system," *Electr. Eng.*, vol. 100, no. 3, pp. 1589–1599, Sep. 2018.

[31] *IEEE Standard for Interconnecting Distributed Resources With Electric Power Systems*, IEEE Standard 1547.2-2008, Apr. 2009, pp. 1–217.

[32] S. A. Eghbali-Khob, M. Moazzami, and R. Hemmati, "Advanced model for joint generation and transmission expansion planning including reactive power and security constraints of the network integrated with wind turbine," *Int. Trans. Electr. Energ. Syst.*, vol. 29, no. 4, pp. 1–20, 2019.

[33] S. A. Bozorgavari, J. Aghaei, S. Pirouzi, A. Nikoobakht, H. Farahmand, and M. Korpås, "Robust planning of distributed battery energy storage systems in flexible smart distribution networks: A comprehensive study," *Renew. Sustain. Energy Rev.*, vol. 123, May 2020, Art. no. 109739.

[34] H. Kiani, K. Hesami, A. Azarhooshang, S. Pirouzi, and S. Safaee, "Adaptive robust operation of the active distribution network including renewable and flexible sources," *Sustain. Energy, Grids Netw.*, vol. 26, Jun. 2021, Art. no. 100476.

[35] S. Mirjalili, S. M. Mirjalili, and A. Lewis, "Grey wolf optimizer," *Adv. Eng. Softw.*, vol. 69, pp. 46–61, Mar. 2014.

[36] H. S. Gill, B. S. Khehra, A. Singh, and L. Kaur, "Teaching-learning-based optimization algorithm to minimize cross entropy for selecting multilevel threshold values," *Egyptian Inform. J.*, vol. 20, pp. 11–25, Mar. 2019.

[37] W. K. A. Najy, H. H. Zeineldin, and W. L. Woon, "Optimal protection coordination for microgrids with grid-connected and islanded capability," *IEEE Trans. Ind. Electron.*, vol. 60, no. 4, pp. 1668–1677, Apr. 2013.

[38] J. Aghaei, N. Amjady, A. Baharvandi, and M.-A. Akbari, "Generation and transmission expansion planning: MILP-based probabilistic model," *IEEE Trans. Power Syst.*, vol. 29, no. 4, pp. 1592–1601, Jul. 2014.

[39] *Nord Pool*. Accessed: Sep. 2020. [Online]. Available: https://www.nordpoolgroup.com/historical-market-data/

[40] A. Askarzadeh, "A novel metaheuristic method for solving constrained engineering optimization problems: Crow search algorithm," *Comput. Struct.*, vol. 169, pp. 1–12, Jun. 2016.

[41] R. R. Rani and D. Ramyachitra, "Krill herd optimization algorithm for cancer feature selection and random forest technique for classification," in *Proc. 8th IEEE Int. Conf. Softw. Eng. Service Sci. (ICSESS)*, Beijing, China, Nov. 2017, pp. 109–113.

[42] IIT Power Group. (2003). *IEEE 118-Bus Test System*. [Online]. Available: http://motor.ece.iit.edu/data/JEAS_IEEE118.doc

[43] L. Baringo and A. J. Conejo, "Strategic wind power investment," *IEEE Trans. Power Syst.*, vol. 29, no. 3, pp. 1250–1260, May 2014.